Stochastic exclusion processes with extended hopping

Ding-wei Huang
Department of Physics, Chung Yuan Christian University, Chung-li, Taiwan
(Received 29 January 2001; revised manuscript received 2 May 2001; published 20 August 2001)

We study the effects of extended hopping in the stochastic asymmetric simple exclusion process (ASEP) of one dimension. A modified ASEP with four parameters is proposed. The current and bulk density are calculated. Two different phases with a curved boundary are observed. The phase of maximum current is absent. We also present the unusual density fluctuations near both boundaries. The characteristic of the stochastic dynamics with extended hopping is pointed out.

DOI: 10.1103/PhysRevE.64.036108 PACS number(s): 05.40.−a, 45.70.Vn

I. INTRODUCTION

Recently the asymmetric simple exclusion processes (ASEP's) in one dimension have been the subject of extensive studies [1]. The simple model serves as a prototype for nonequilibrium systems and has attracted a lot of interest for its many applications [2]. It is well known that one-dimensional systems with short-range interactions do not exhibit phase transition in thermal equilibrium. However, when the systems are driven out of equilibrium, many interesting phenomena emerge. Steady current is established in stationary states. Shocks emerge spontaneously. Bulk properties can be changed by a small variation of the boundary conditions. Such boundary-induced phase transitions may occur in a wide class of driven systems, e.g., in biological mechanisms [3], sociological interactions among agents, or traffic flow of highway [4]. The study of ASEP would lead to a better understanding of such phenomena, which cannot be described in the framework of equilibrium statistical mechanics.

The basic model describes driven lattice gases in one dimension with hard-core repulsion, i.e., only the nearest-neighbor hopping is considered. This kind of short-range interaction provides an additional particle-hole symmetry, which dictates the collective behavior. For some models, such symmetry leads to the exact results for stationary states [5]. In Ref. [6], the next-nearest-neighbor interaction is considered. However, particles are still restricted to nearest-neighbor hopping, where the hopping rate is determined by the configuration of the next-nearest-neighbor site. It would be interesting to study the effects of extended hopping, which violates the particle-hole symmetry. In Ref. [7], the extended hopping is discussed in the deterministic ASEP. Strong fluctuations of density over lattice sites are observed. Another essential extension of the basic model is to include the stochastic noise [8]. The fluctuations caused by such noise are inevitable and important in the nonequilibrium phenomena. The effects of stochastic noise are most often discussed within the framework of nearest-neighbor hopping. The main aim of this paper is to study the combining effects of stochastic noise and extended hopping in ASEP.

The paper is organized as follows. The model is described in Sec. II. In Sec. III we study the properties in bulk. Both the current and bulk density are calculated. In Sec. IV we analyze the density profiles. The distributions near the boundaries are studied in detail. The results are summarized in Sec. V with some conclusions.

II. MODEL

Consider a one-dimensional lattice of L sites with open boundaries. Particles are introduced into the system at the left end (site 1), move through the bulk, and leave the system at the right end (site L).

Within the bulk, particles move according to the dynamics prescribed by the Nagel-Schreckenberg traffic model [4]. Each site is either empty or occupied by a particle with velocity v, which is an integer ranging from 0 to v_{max}. The parameter v_{max} denotes the maximum velocity. Particles are confined to move in one direction only. The configurations are updated synchronously according to the following successive steps: (1) Acceleration—increase v by 1 if $v < v_{max}$. (2) Slowing down—decrease v to d if $v > d$, which denotes the number of empty sites in front of the particle. (3) Stochasticity—if $v > 0$, further decrease v to $v-1$ with a probability p. (4) Movement—hop v sites forward.

The dynamics are controlled by two parameters: v_{max} and p. In the case of $v_{max}=1$, the model reduces to the well-known ASEP. When $p=0$, particles hop one site to the right if the site in front of them is empty, which is known as deterministic ASEP; when $p>0$, particles may stay motionless even if empty sites are available, which is then known as stochastic ASEP. Usually the ASEP is studied with a random sequential update. In this paper, we consider the parallel update, which provides much stronger correlations among particles. A comparison of different update procedures can be found in Ref. [9]. The extended hopping is implemented with $v_{max}>1$, where particles are allowed to hop more than one site within a single time step.

The boundary conditions are specified as follows. The two ends of the system are taken as coupled to two stochastic reservoirs. Particles are injected at the left end with probability α, provided the first site (site 1) is empty; particles are removed at the right end with probability β, provided the last site (site L) is occupied. In this paper, we simply adopt the constraints that the injected particle has the maximum velocity v_{max} and particles are not allowed to leave the system without stopping at the last site. It can be achieved by sitting a stationary particle at site $L+1$. The model is characterized by four parameters: two at the ends (α and β) and two in the

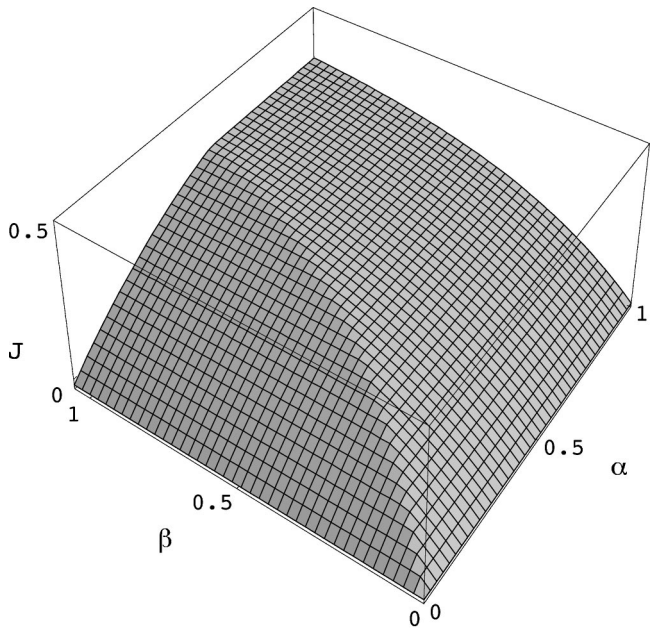

FIG. 1. Current J as a function of rates α and β. The parameters are $p=0.3$ and $v_{max}=2$.

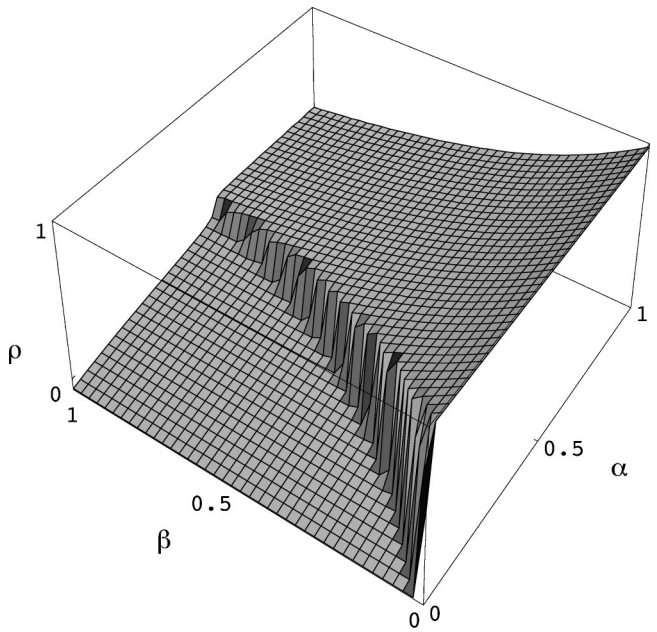

FIG. 2. Bulk density ρ as a function of rates α and β. The parameters are $p=0.3$ and $v_{max}=2$.

bulk (v_{max} and p). The extended hopping is realized by a maximum velocity larger than 1. The other three parameters are stochastic probabilities at the boundaries and in the bulk.

III. CURRENT AND BULK DENSITY

First, we study the current J and bulk density ρ as functions of boundary rates α and β; v_{max} and p are fixed parameters. As the boundary rates α and β change, three different phases can be observed: the high-density phase, the low-density phase, and the maximum current phase. The maximum current phase can be reached only in the case of $p>0$ and $v_{max}=1$, where all three different phases can be observed; in other cases, only the high-density phase and the low-density phase are observed. In the case of $p=0$, the phase transition is observed along the line of equal rates $\alpha=\beta$ and independent of v_{max} [7]. In the case of $p>0$ and $v_{max}=1$, the transition between the high-density phase and the low-density phase is still along the same straight line. The domain of the high-density phase is equal to that of the low-density phase. A symmetry between two rates, α and β, is observed. In contrast, in the case of $p>0$ and $v_{max}>1$, the domain of the high-density phase expands with the shrinkage of the low-density domain. The resulting current J and bulk density ρ are shown in Figs. 1 and 2, respectively. In the high-density phase, the current J and the bulk density ρ are controlled by the removal rate β and independent of the injection rate α. To the contrary, in the low-density phase, the distribution is controlled by α and independent of β. The phase transition line is no longer a straight line in the (α,β) plane, see Fig. 3. When α and β are small, the phase boundary approaches the line of $\alpha=\beta$. As the rates increase, the boundary deviates from the straight line $\alpha=\beta$ and curves toward the β axis. The convexity, i.e., the boundary bends upward, and increases with the increase of p. In the case of a large p, i.e., $p\sim1$, the high-density phase becomes dominant. The low-density phase can only be observed within a small region confined by a very small α. The location of the phase boundary is mainly determined by the parameter p as long as $v_{max}>1$. In the special case of $p>0$ and $v_{max}=1$, the maximum current phase can be reached when both the rates are larger than a critical value of $(1-\sqrt{p})$. The phase boundaries

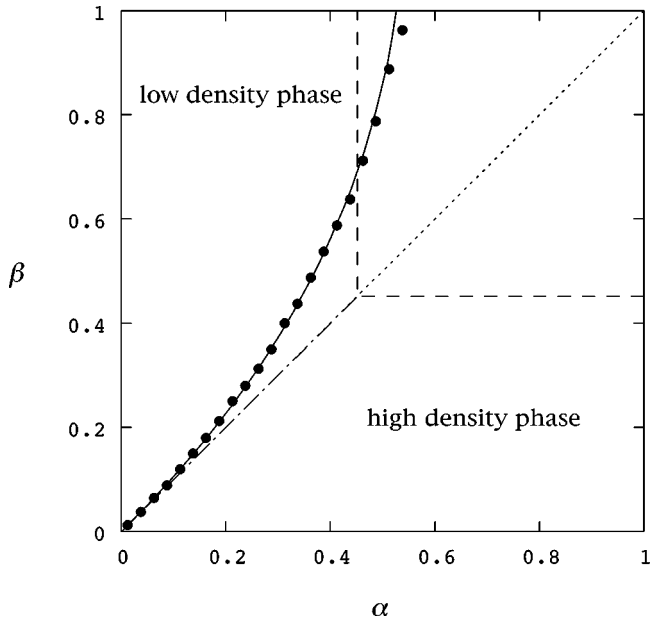

FIG. 3. Phase diagram in the (α,β) plane. The parameters are $p=0.3$ and $v_{max}=2$. Data points are the phase boundary. The result from the fundamental diagram is shown by the solid line. The boundary in the case of $p=0$ is shown by the dotted line; the boundaries in the case of $p=0.3$ and $v_{max}=1$ are shown by the dash lines.

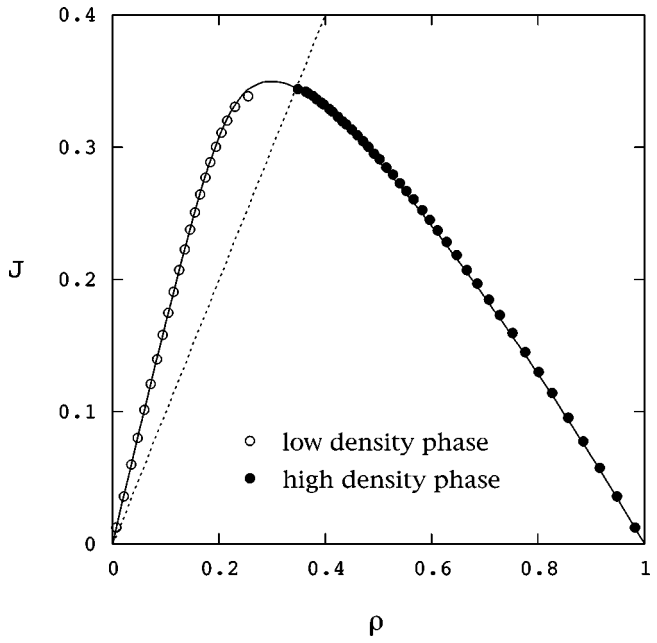

FIG. 4. Current J as a function of bulk density ρ. The parameters are $v_{max}=2$ and $p=0.3$. The open circles are the data from low-density phase; the closed circles are the data from high-density phase. The fundamental diagram $J_0(\rho)$ is shown by the solid line. The dotted line shows $J=\rho$.

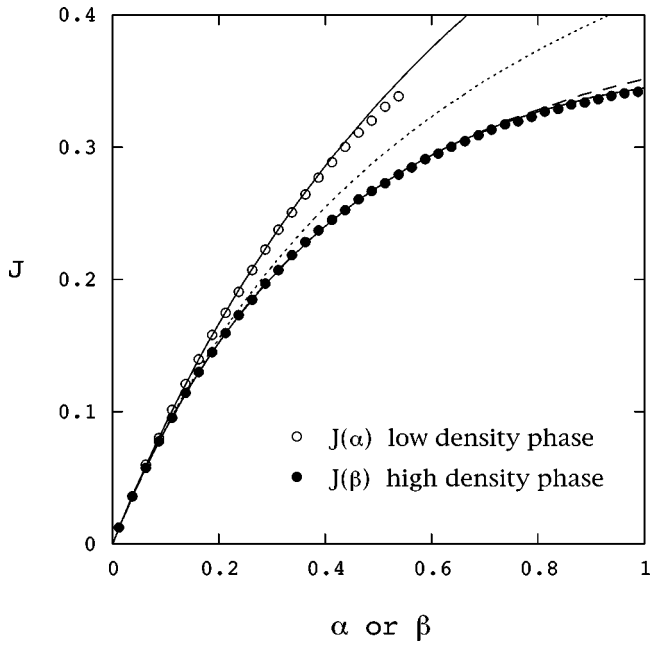

FIG. 5. The characteristic current J as a function of boundary rate α or β. The parameters are $p=0.3$ and $v_{max}=2$. The open circles show $J(\alpha)$ in the low-density phase; the closed circles show $J(\beta)$ in the high-density phase. The results from the fundamental diagram are shown by the solid lines. The result from the simple mean-field approximation in the high-density phase is shown by the dotted line; the dash line shows the result including the next order correction.

become straight lines again, see Fig. 3.

Across the phase transition line, the current J is continuous while a discontinuity is developed in the bulk density ρ. As the phase transition is induced by the boundaries, one expects the same relationship between the current J and bulk density ρ as in the case of periodic boundary conditions, which is known as the fundamental diagram $J_0(\rho)$. The results are shown in Fig. 4. It is clearly shown that all the data, for various α and β, collapse into the fundamental diagram and the maximum current has never been achieved. The maximum value of the achieved current is observed at the maximum removal rate $\beta=1$. Its value is mainly determined by the parameter p and can be well reproduced by a simple expression $(1-p)/2$.

In the high-density phase, particles are crowded together and the current is controlled by the removal rate β. A flat density profile near the right end (site L) is expected. The constraint on a constant current gives $J=J_0(\rho)=\rho\beta$. After inverting the fundamental diagram in the high-density part, the characteristic relation $J(\beta)$ between the current and the removal rate can then be obtained, see Fig. 5. The maximum value of the current can also be correctly reproduced at the intersection of the fundamental diagram and the line of the maximum removal rate $J=\rho$, see Fig. 4. In the special case of $p=0$, we have $J_0(\rho)=1-\rho$. Both the current and bulk density are independent of v_{max}. When $p>0$, a small dependence on v_{max} from $J_0(\rho)$ is expected. The simple mean-field approximation gives $J_0(\rho)\sim(1-p)(1-\rho)$. However, failing to include the v_{max} dependence, the approximation provides a satisfactory description to the fundamental diagram only in the very high-density limit. Thus the resulting characteristic relation $J=\beta(1-p)/(1-p+\beta)$ is valid only when β is small. The dependence on v_{max} becomes obvious when β is large. The inclusion of the next order correction, the order of $(1-\rho)^2$, will lead to a satisfactory result, see Fig. 5.

Similarly, in the low-density phase, particles move with an average speed $\langle v\rangle>1$ and the current is controlled by the injection rate. The constraint on a constant current on the left end (site 1) gives $J=J_0(\rho)=(1-\rho_1)\alpha$, where ρ_1 is the average density on the first site. With $\langle v\rangle>1$, the bulk density assumes a smaller value than ρ_1 and can be expressed as $\rho=\rho_1/\langle v\rangle$. The characteristic relation $J(\alpha)$ is then given by $J=\alpha/(1+\alpha)$. It is interesting to note that the current is independent of v_{max} and can be readily reproduced by the simple mean-field approximation $J_0(\rho)=(v_{max}-p)\rho$.

There are two characteristic relations: $J(\beta)$ in the high-density phase and $J(\alpha)$ in the low-density phase. In the case of $p=0$, these two characteristic relations coincide. The current increases with the increase of the boundary rate. In the low-density phase, particles move independently. Introducing the stochastic noise does not provide any difference; except reducing the average speed from v_{max} to $v_{max}-p$. The same current can still be achieved at the same injection rate. As the average speed decreases a bit, the resulting bulk density increases a bit accordingly. In the high-density phase, particles are strongly correlated. The stochastic noise has a much more significant influence. At the same removal rate β, the current decreases with the increase of noise. The current still increases monotonically with the increase of p, but at a much slower rate. As p increases, the curve $J(\beta)$ bends to

lower values; while the curve $J(\alpha)$ remains the same. The matching condition of equal current $J(\alpha)=J(\beta)$ prescribes a curved phase boundary as shown in Fig. 3.

It is interesting to further note that an increment on the maximum velocity will not lead to a larger value of current, as naively expected. The distributions of the high-density phase are mainly determined by the stochastic noise p. Only a weak dependence on v_{max} is observed. In the low-density phase, the current is independent of both p and v_{max}. The value of the bulk density decreases with the increase of v_{max}. Thus the discontinuity at the transition increases with the increase of v_{max}.

IV. DENSITY PROFILE

Next, we consider the density profiles. As the current is controlled by one of the boundary rates, the density profile is expected to be flat except near the other boundary. In the high-density phase, a flat profile except near the left end is expected; in the low-density phase, a flat profile except near the right end is expected. Such expectation is realized in the case of $v_{max}=1$, for both $p=0$ and $p>0$. A flat density profile in the bulk and through one of the boundaries is observed; near the other boundary, the density profile changes monotonically from the bulk density to the value at the boundary. In the case of $v_{max}>1$ and $p=0$, the average densities divide into two branches according to their locations. Unusual density fluctuation between these two branches is observed. In the high-density phase, the fluctuation is limited to a boundary layer near the left end. A flat profile is still observed in the bulk and through the right end. In the low-density phase, the fluctuation can be observed all through the bulk, except near the right end. The flat profile is replaced by strong fluctuation between two flat branches. With stochastic noise, i.e., $v_{max}>1$ and $p>0$, the fluctuation diminishes. A flat density profile is restored in the bulk, while interesting fluctuation is developed near both boundaries.

In the low-density phase, the removal of a particle is much more effective than its insertion. The current is determined by the injection rate α and a flat density profile is expected in the bulk and through the left end. However, in the case of $v_{max}>1$ and $p>0$, an interesting fluctuation is observed near the left end, see Fig. 6. As α increases, the bulk density increases accordingly; while the pattern of fluctuation remains the same. A rescale of the density will lead to the same profile for different values of α, which can be well reproduced by the following phenomenological considerations. The average density on the first site is determined by $\rho_1=1-J/\alpha$. As the particle is injected with a speed of $v_{max}=2$, we have $\rho_2=p\rho_1$, i.e., only the effect of stochastic noise will let a particle stop at the second site. In the low-density phase, a particle keeps its speed at $v_{max}=2$ and hops to the neighbor site with a probability p or to the next neighbor site with a probability $(1-p)$. Thus we have $\rho_i=p\rho_{i-1}+(1-p)\rho_{i-2}$ for $i\geqslant 3$. The results are shown in Fig. 6. After a few oscillations, the densities approach the asymptotic value ρ. The pattern of oscillations is controlled by the stochastic noise p. The ratio ρ_1/ρ is a constant determined by p and independent of α, which results in the scaling behavior for various α. A simple expression is obtained as $\rho_1/\rho=\langle v\rangle=v_{max}-p$. With a large noise, $p\sim 1$, the ratio ρ_1/ρ approaches a value of 1. The fluctuation is smeared out by the stochastic noise. The densities reach the asymptotic value quickly and only a few oscillations can be observed. With a small noise, $p\sim 0$, many oscillations can be observed before the densities reach the bulk value. The ratio ρ_1/ρ approaches a value of 2. In the limiting case of $p=0$, the oscillations continue all through the bulk. As the densities alternate by sites, a coarse-grained average is assigned to the bulk density at a value of $\rho_1/2$.

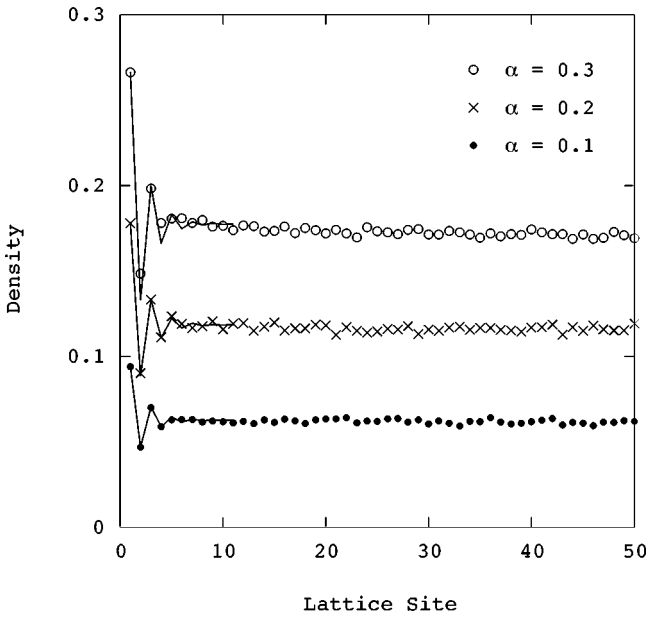

FIG. 6. Density profile ρ_i as a function of site i near the left end for various α. Parameters $v_{max}=2$, $p=0.5$, and $L=2000$; the low-density phase is assumed. The results are independent of β. Solid lines show the predictions from phenomenological considerations.

Near the left end and in the bulk, the densities are determined by α and independent of β; the influence of β can only be observed near the right end. The density on the last site is given by $\rho_L=J/\beta$, which is always larger than the corresponding bulk density. Thus the densities are expected to increase monotonically as one approaches the right end. With a larger β, a slower increase is predicted. However, the densities increase smoothly only up to the site $L-1$. On the last site (site L), a sudden drop of density is observed, see Fig. 7. Just like the oscillations near the left end, the abrupt drop of density on the last site is also a characteristic of stochastic noise. Such interesting behavior has a clearer manifestation in the high-density phase.

In the high-density phase, particles are inserted much more efficiently than they are removed. Thus the current is determined by the removal rate β. When β is small, a flat profile is observed through the right end as expected. As β increases, the flat profile in the bulk assumes a lower value as the removal rate becomes more efficient. It is interesting to observe that the average density on the last site ρ_L assumes an even lower value than the bulk density ρ. A sudden drop of density on site L is observed. The difference between ρ

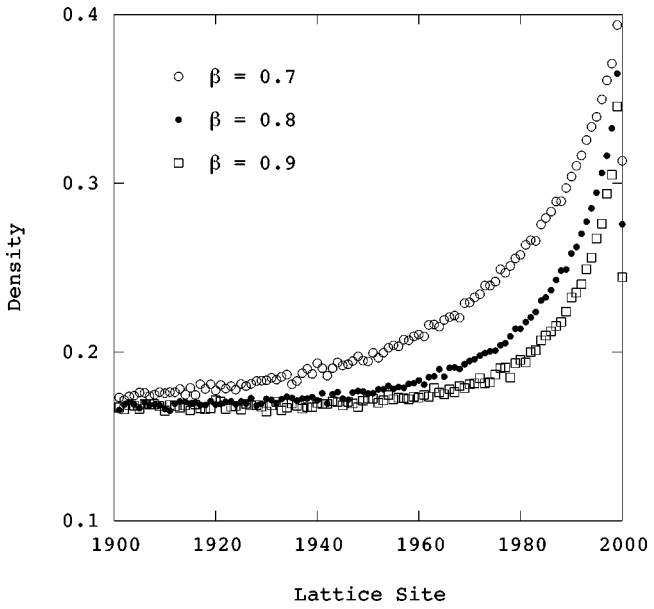

FIG. 7. Density profile ρ_i as a function of site i near the right end for various β. Parameters $\alpha=0.3$, $v_{max}=2$, $p=0.5$, and $L=2000$; the low-density phase is assumed.

and ρ_L increases with the increase of β. As β further increases, particles begin to accumulate near the right end. The densities have a quick rise just before the boundary, followed by an abrupt drop on the boundary, see Fig. 8. This peculiar behavior can be attributed to the combined effect of extended hopping and stochastic noise. When $v_{max}=1$ or $p=0$, we have $\rho_L=\rho$ in the high-density phase. The pattern of density fluctuation is mainly controlled by the parameter p. Only weak dependence on v_{max} is observed, as long as $v_{max}>1$. As p increases, the pattern of oscillations becomes more

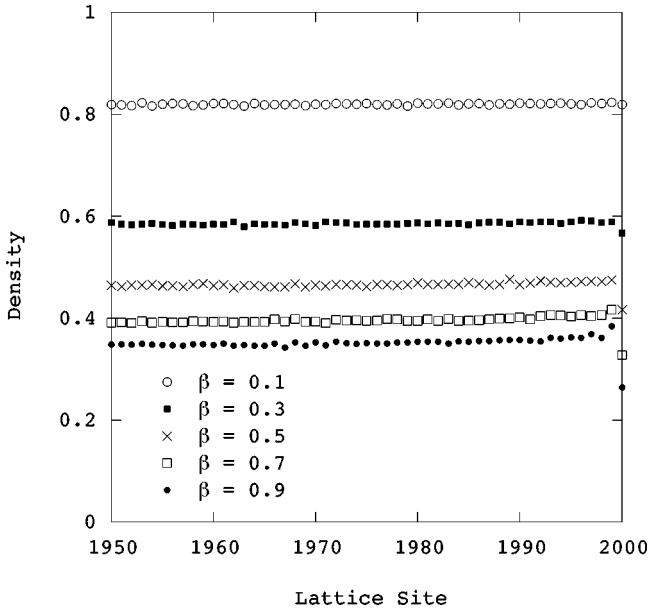

FIG. 8. Density profile ρ_i as a function of site i near the right end for various β. Parameters $v_{max}=2$, $p=0.5$, and $L=2000$; the high-density phase is assumed. The results are independent of α.

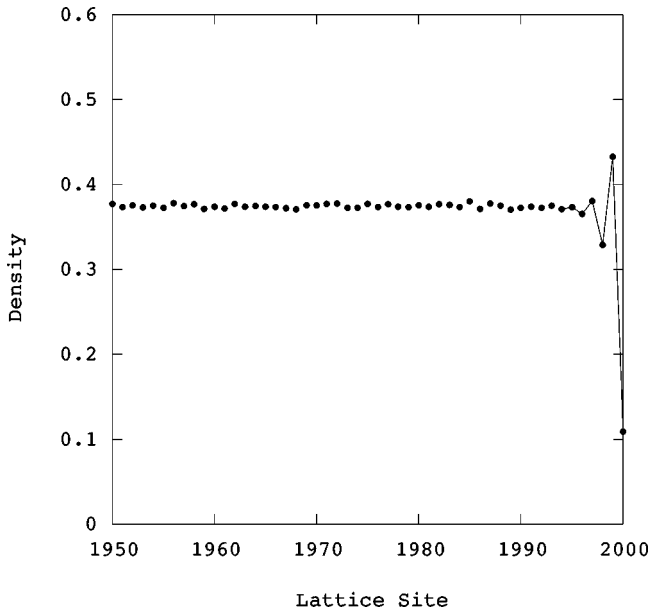

FIG. 9. Density profile ρ_i as a function of site i near the right end. Parameters $\alpha=0.5$, $\beta=0.9$, $v_{max}=2$, $p=0.8$, and $L=2000$; the high-density phase is assumed. The solid line shows the oscillations.

clear, see Fig. 9. Basically, it's the counterpart of the oscillations observed in the low-density phase, see Fig. 6. Both can be taken as the characteristic manifested only in the case of $v_{max}>1$ and $p>0$.

As expected, the influence of α can be observed in the density distribution near the left end. The average density on the first site is given by $\rho_1=1-J/\alpha$. When α is small, ρ_1 is less than ρ; when α is large, ρ_1 is larger than ρ. This provides a criterion to divide the high-density phase into two subphases. The same feature also appears in the case of $v_{max}=1$ and $p>0$. It is interesting to note that in the case of $p=0$, for both $v_{max}=1$ and $v_{max}>1$, ρ_1 is always smaller than ρ, and only one of the subphases can be reached. In the case of $v_{max}=1$ and $p>0$, the average densities change monotonically as one approaches the left end. However, in the case of $v_{max}>1$ and $p>0$, the pattern of oscillations is again observed near the boundary, see Fig. 10. In the extreme cases of very small α or very large α, the oscillations disappear and the profiles become monotonic functions, as in the case of $v_{max}=1$ and $p>0$. The effect of extended hopping is observed in an unusual fluctuation of densities near the left end. The average densities fluctuate within a boundary layer before they converge into a smooth profile. As the stochastic noise decreases, the convergence becomes slower and more oscillations can be observed. In the limit of $p=0$, the very slow convergence can be reinterpreted as fluctuations between two branches.

V. CONCLUSION

In this paper, we study the effects of extended hopping and stochastic noise in asymmetric simple exclusion process. Parameter $v_{\max}>1$ provides the possibility for a particle to move more than one site within a single time step. Parameter

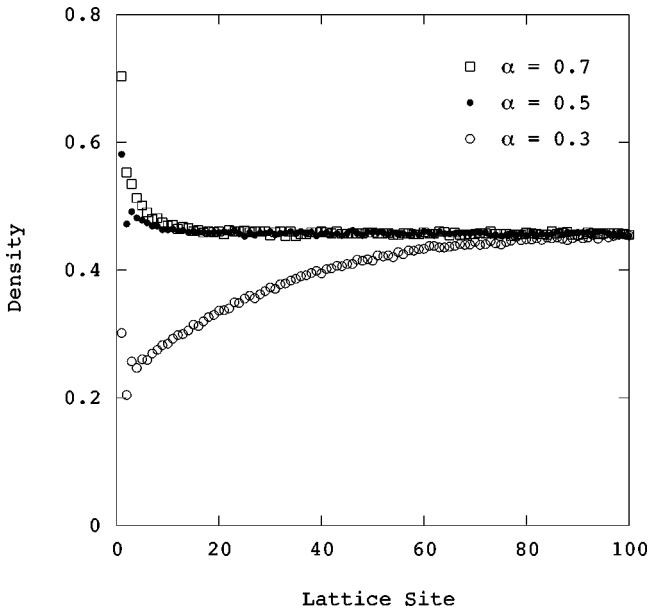

FIG. 10. Density profile ρ_i as a function of site i near the left end for various α. Parameters $\beta=0.5$, $v_{max}=2$, $p=0.5$, and $L=2000$; the high-density phase is assumed.

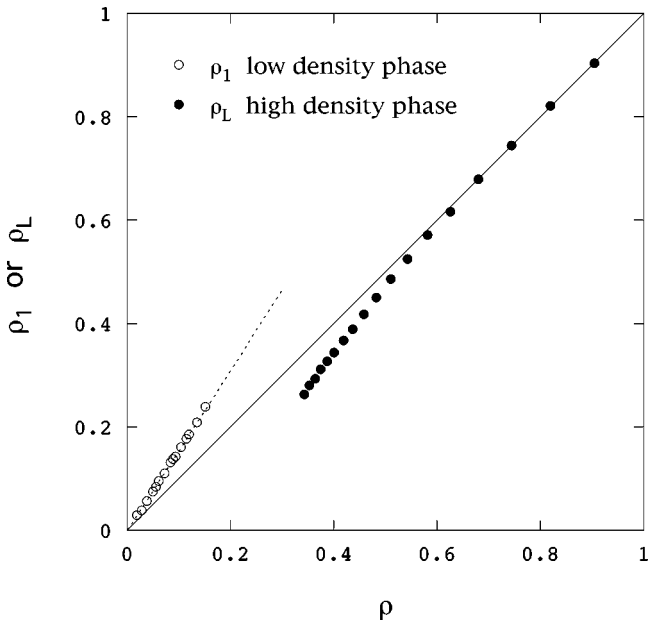

FIG. 11. Densities on the boundaries ρ_1 and ρ_L as functions of the bulk density ρ. Parameters $v_{max}=2$, $p=0.5$, and $L=2000$. The open circles are the data from the low-density phase; the closed circles are the data from the high-density phase. The solid line shows $\rho_1=\rho$ or $\rho_L=\rho$; the dashed line shows $\rho_1/\rho=v_{max}-p$ in the low-density phase.

$p>0$ introduces the possibility for a particle to stay motionless when no other particles obstructed the way. In contrast to the deterministic ASEP, both the boundary conditions and the dynamics are stochastic, which are controlled, respectively, by three different parameters α, β, and p.

We observe two distinct phases: the low-density phase and the high-density phase. The phase of maximum current is absent. Even with a high injection rate, a high removal rate, and assigning the injected particle with a high speed, the maximum current has never been achieved. The two phases resulted from the competing of two rates on the boundaries. The less efficient boundary determined the current and bulk density. In the high-density phase, the properties in bulk are controlled by the removal rate; in the low-density phase, the injection rate controls the results. The observed properties can be understood from the fundamental diagram with simple phenomenological considerations. The location of the phase boundary can also be deduced. Various features are mainly determined by the parameter p; the parameter v_{max} only has a minor influence as long as $v_{max}>1$. However, the features observed in the case of $v_{max}>1$ are distinctly different from those of $v_{max}=1$. With nearest-neighbor hopping, an additional symmetry between a particle and an empty site is observed. With extended hopping, this symmetry is no longer applied.

The density profile has a flat distribution except near both boundaries. Interesting oscillations of densities near both boundaries are observed, which provide a characteristic to the combination of extended hopping and stochastic noise, i.e., $v_{max}>1$ and $p>0$. When $v_{max}=1$ or $p=0$, the density profile has a flat distribution through one of the boundaries, i.e., the one with less efficiency. Figure 11 shows the average density on the less efficient boundary. When $v_{max}=1$ or $p=0$, we have $\rho_1=\rho$ in the low-density phase and $\rho_L=\rho$ in the high-density phase. Deviation from such behavior is observed and becomes a characteristic to the stochastic dynamics with extended hopping. In the low-density phase, the ratio ρ_1/ρ is a constant larger than 1. In the high-density phase, the ratio ρ_L/ρ is less than 1 and varies with the density. The ratio approaches 1 only when the density is high. This behavior provides an interesting example to the boundary-induced phase transitions. In such cases, the properties of phase transition are controlled by the specifications of boundary conditions. With the same dynamics, a different choice of boundary conditions will lead to a different phase diagram [8]. It would be interesting to further study the relation between the resulting phase diagram and the chosen boundary condition.

[1] B. Derrida, Phys. Rep. **301**, 65 (1998).

[2] *Nonequilibrium Statistical Mechanics in One Dimension*, edited by V. Privman (Cambridge University, Cambridge, 1997).

[3] J. T. MacDonald and J. H. Gibbs, Biopolymers **7**, 707 (1969); G. M. Schütz, Int. J. Mod. Phys. B **11**, 197 (1997).

[4] K. Nagel and M. Schreckenberg, J. Phys. I **2**, 2221 (1992); M. Schreckenberg, A. Schadschneider, K. Nagel, and N. Ito, Phys. Rev. E **51**, 2939 (1995).

[5] G. M. Schütz and E. Domany, J. Stat. Phys. **72**, 277 (1993); A. Honecker and I. Peschel, *ibid.* **88**, 319 (1997); M. R. Evans, N.

Rajewsky, and E. R. Speer, *ibid.* **95**, 45 (1999); J. de Gier and B. Nienhuis, Phys. Rev. E **59**, 4899 (1999).
[6] T. Antal and G. M. Schütz, Phys. Rev. E **62**, 83 (2000).
[7] D. W. Huang, Phys. Rev. E **63**, 012 104 (2001); S. Cheybani, J. Kertész, and M. Schreckenberg, *ibid.* **63**, 016 107 (2001).
[8] S. Cheybani, J. Kertész, and M. Schreckenberg, Phys. Rev. E **63**, 016 108 (2001).
[9] N. Rajewsky, L. Santen, A. Schadschneider, and M. Schreckenberg, J. Stat. Phys. **92**, 151 (1998).